Machine Vision–Based Guidance System for an Agricultural Small-Grain Harvester

Article · July 2003

DOI: 10.13031/2013.13945

3 authors:

Eric Randolph Benson
University of Delaware
56 PUBLICATIONS **453** CITATIONS
SEE PROFILE

John Franklin Reid
John Deere
132 PUBLICATIONS **1,762** CITATIONS
SEE PROFILE

Quanyi Zhang
Northwestern Polytechnical University
48 PUBLICATIONS **851** CITATIONS
SEE PROFILE

MACHINE VISION–BASED GUIDANCE SYSTEM FOR AN AGRICULTURAL SMALL–GRAIN HARVESTER

E. R. Benson, J. F. Reid, Q. Zhang

ABSTRACT. *A machine vision guidance system was developed for an agricultural combine harvester. The guidance algorithm separated the uncut crop rows from the surrounding background material, parameterized the crop rows, and calculated a guidance signal. A single monochrome camera mounted on the cab of the combine supplied the crop images. The algorithm was developed for corn and was tested under both laboratory and field conditions. Test results showed that the algorithm was capable of accurately locating crop rows in the image and providing a satisfactory lateral position signal for automated combine guidance. At a speed of 1.3 m/s (3 mph), the system was capable of guiding the combine at the same accuracy level as the GPS recording system available.*

Keywords. *Automatic guidance, Automatic steering, Automation, Combine harvesters, Control, Controllers, Corn, Fuzzy logic, GPS, Harvesters, Harvesting, Image processing, Image processors, Machine vision.*

Interest in agricultural guidance is driven by economic, ergonomic, and social factors. Automatic guidance systems have the potential to reduce the number of operations in the field, improve efficiency, and minimize compaction, leading to improved yield and profitability (Gan–Mor and Clark, 2001). Minimizing overlap, for example, decreases the number of passes required in the field and reduces the amount of time and fuel required to accomplish the task. The national trend has been a decline in the number of farms but an increase in the size of farms. To cover an increasing area with a decreasing labor force, owners have moved to larger, higher capacity equipment.

The operator is one of the greatest limitations to increased vehicle performance (Fitzpatrick et al., 1997). The operator's primary task is to supervise the field operation, with steering requiring a high level of concentration and having a large impact on quality (Jahns, 1997; Van Zuydam, 1999). Increasing operating speed and vehicle size requires that the operator to devote more time to steering, leaving less attention available for implement performance (Wilson, 2000). Fatigue plays an important role, especially during the tight time constraints of harvest. New sensors and guidance systems can open opportunities for nighttime operation (Nieminen and Sampo, 1993). Automatic guidance has the potential to reduce operator fatigue and improve vehicle positioning accuracy (Gerrish et al., 1997). Estimates have shown that an improved navigation system could reduce up to 10% of field crop production costs (Palmer and Matheson, 1988).

Vehicle automation has been simplified by improvements in vehicle technology. The increasing use of electrohydraulics has greatly enhanced vehicle control. Advancements in technology make automatic guidance more practical today than when first proposed (Callaghan et al., 1997). Increased emissions requirements have forced most agricultural machinery companies to adopt electronically controlled engines and transmissions. The controller area network (CAN–bus) provides a foundation for information exchange between various vehicle systems (Reid et al., 2000).

Sensor and computer costs have declined, while capability and functionality have increased. The price of GPS receivers has decreased, while the accuracy has increased. Industries, such as maritime, aviation, and shipping, increasingly rely on differential GPS. Embedded vehicle controls are used for a myriad of automotive applications, helping to decrease the cost for allied industries such as agriculture.

A number of agricultural guidance technologies have been developed or demonstrated in recent years, with tractor guidance receiving the primary emphasis. Technologies such as machine vision, GPS, inertial positioning systems, and sensor fusion systems have been utilized to control the path and operation of the tractor in the field, enhancing planting, cultivation, and other operations. Researchers at the National Robotics Engineering Consortium developed a windrower that utilized electronic differential drive control and machine vision technology to successfully cut alfalfa under typical field conditions (Ollis, 1997; Ollis and Stentz, 1996; Fitzpatrick et al., 1997). More recently, Keicher and Seufert

Article was submitted for review in January 2002; approved for publication by the Information & Electrical Technologies Division of ASAE in March 2003.

Published as Paper No. 02–02–1721 in the Journal Series of the Delaware Agricultural Experiment Station.

Case IH is a trademark of CNH Global NV. Mention of trade names, proprietary products, or specific equipment does not constitute a guarantee or warranty by the University of Delaware, the University of Illinois, or Deere and Company, and does not imply the approval of the named product to the exclusion of other products that may be suitable.

The authors are **Eric R. Benson, ASAE Member Engineer,** Assistant Professor, Delaware Experimental Station, Department of Bioresources Engineering, University of Delaware, Newark, Delaware; **John F. Reid, ASAE Member Engineer,** Manager, Intelligent Vehicle Systems, Deere and Co., Champaign, Illinois; and **Qin Zhang, ASAE Member Engineer,** Assistant Professor, Department of Agricultural Engineering, University of Illinois, Urbana, Illinois. **Corresponding author:** Eric Benson, 242 Townsend Hall, University of Delaware, Newark, DE 19717–1303; phone: 302–831–0256; fax: 302–831–2469; e–mail: ebenson@udel.edu.

  ISSN 0001–2351

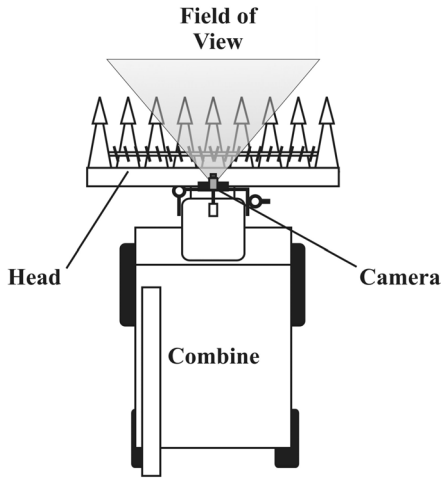

Figure 1. Monochrome camera located above the cab of the combine.

(2000) developed a vision–based hoe guidance system for cultivation that was capable of 5.0 cm accuracy at 3.5 m/s. Agricultural machine vision guidance systems have been demonstrated under typical field conditions at 4.7 m/s on straight rows and 2.7 m/s on curved rows (Reid et al., 2000). Bell (2000) demonstrated high accuracy (<1 cm mean error) tractor guidance along a predefined path utilizing a four–antenna carrier–phase GPS system. Hague and Tillett incorporated machine vision and inertial sensors on a sprayer robot (Hague and Tillett, 1995; Tillett et al., 1998). The system was capable of selectively spraying at 0.7 m/s and had a mean error of 1 mm along the row and 11 mm lateral error. The research projects described demonstrated different guidance technologies and explored the feasibility of agricultural vehicle guidance.

In this project, a machine vision–based guidance system was developed for grain harvesting. The guidance system controlled the steering of the vehicle during harvesting, but did not include end–of–row turning or transport. Three sensor locations (low on the outside of the head, directly above the crop on the head, and above the cab) were studied. Preliminary results from the system utilizing cameras located low on the head were provided in Benson et al. (2000a, 2000b). The location of the sensor is critical because the location dictates the appearance of the agricultural scene. The appearance of the scene, in turn, determines the guidance algorithm. The optimal location would allow reliable extraction of the guidance directrix under all conditions without compromising or interfering with normal operation. This article details the algorithm used in conjunction with a single camera mounted above the cab, as shown in figure 1.

Objectives

The objectives of this study were:

- Develop a machine vision–based guidance system for grain combines, specifically corn.
- Evaluate the proposed guidance system under both laboratory and typical field conditions for the region.

Camera Location Effects

Camera location has a number of practical and theoretical effects on the guidance algorithm. Ideally, the system would use only a single camera to view the scene. The camera would be located on the combine and would not require any adjustments or calibration changes during the course of the season.

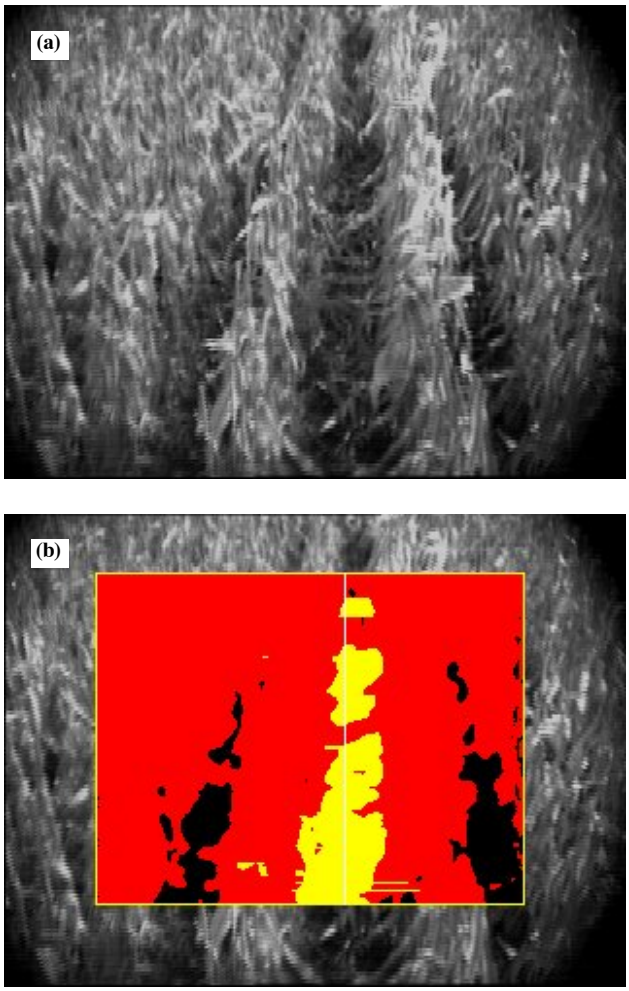

Figure 2. Representative images from the cab mounted camera: (a) unprocessed image, and (b) processed image.

A cab–mounted camera can view more rows than a head–mounted camera. The additional rows provide robustness against crop damage. The height of the crop restricts the row detection ability of the system. With a short, narrow crop, it is possible to separate the crop rows. By harvest, mature corn has often reached a height of 2 m or more, and it can become increasingly difficult to visually separate the individual rows. In tall crops, it is generally possible to locate the space between the center two rows, but it is more difficult to reliably discriminate all of the rows in view. Potential solutions include: (a) utilize the space between the rows for guidance, or (b) use the cut/uncut edge for guidance.

The operator typically drives the vehicle by monitoring the position of the center snout on the corn head relative to the inter–row space. As the width of the combine increases, it becomes difficult for an operator – or a single camera – to see the outer edges of the head. Limiting the field of view of the image sensor decreases the number of rows that can be seen in the image. As the field of view is decreased, the effect of damaged or missing plants increases. With a small field of view, approximately wide enough for two rows, an anomaly in either row can prevent the extraction of accurate guidance

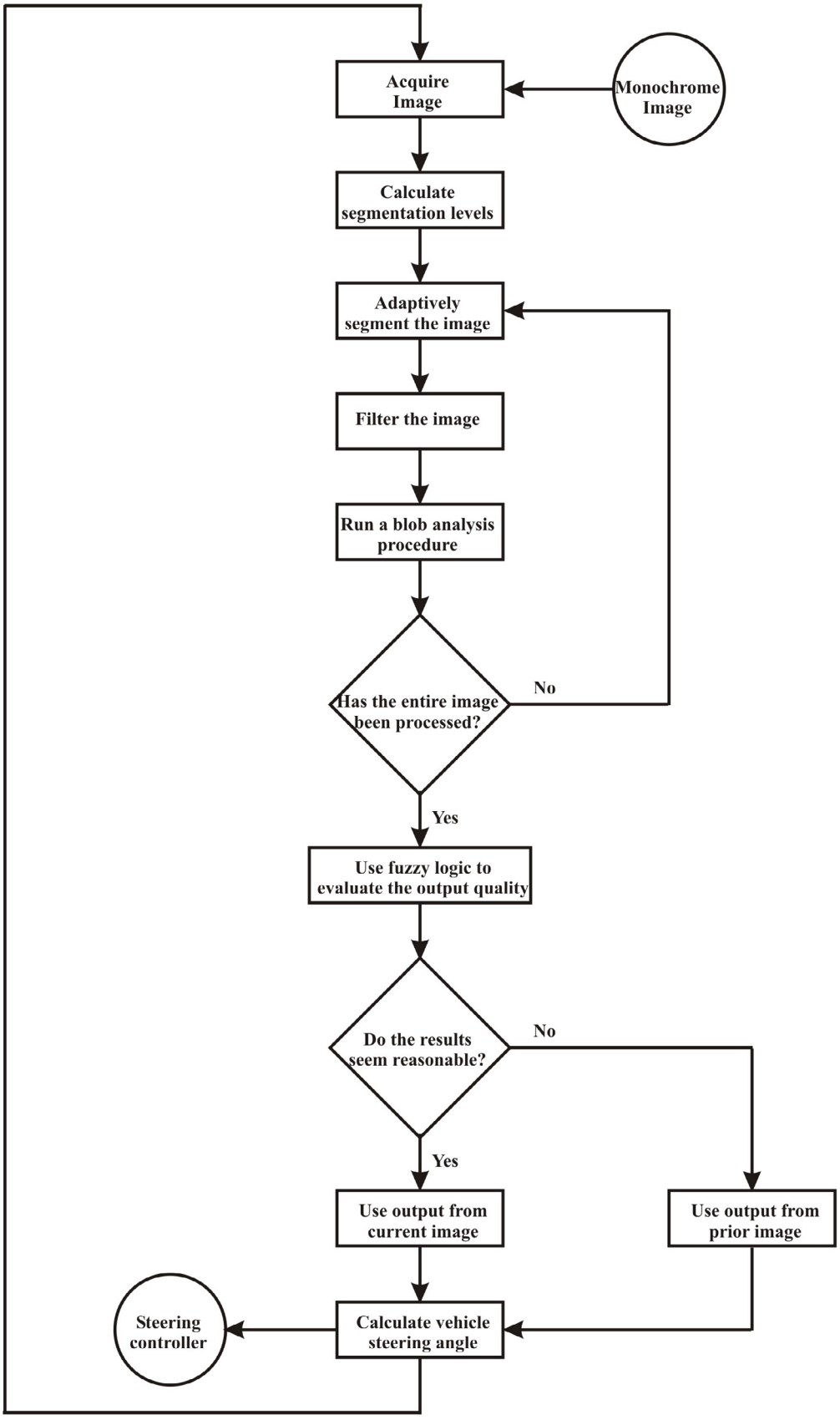

Figure 3. Flowchart of the guidance algorithm.

parameters. As the field of view increases, the amount of information increases, but the ability to process the information decreases.

Shadows and real–world lighting complicate feature parameterization. With a high–mounted camera, crop shadows increase the effective contrast between the crop and inter–row space. The shadow of the combine itself can mask the features of interest during certain combinations of lighting and orientation.

Images from a cab–mounted monochrome camera (fig. 2) can be divided into crop and non–crop regions. The idealized crop row location is based on the location of the camera relative to the feeder assembly. The inter–row space is located from the two rows closest to the center of the combine. The feeder assembly dictates the location and entry angle of the corn plants into the combine. The crop heading angle and offset constitute the error signal on which guidance is based.

Algorithm Description

A flowchart for the algorithm is shown in figure 3. An image was acquired from the image sensor, digitized by the frame grabber, and extracted to memory. An adaptive module determined the appropriate segmentation level for the image. The image was processed from the bottom to the top, starting with segmentation, line–by–line filtering, and then blob analysis. After processing the entire image, the blob statistics (including the area, perimeter, and form factor) were calculated. The guidance signal was calculated from the centroid or regression on the largest blob. A separate fuzzy guidance module evaluated the signal to confirm that the proper crop row had been selected for guidance. A PID controller was used to calculate the actuator command signal from the heading offset. The algorithm is described in more detail below.

The algorithm began by acquiring the image from the sensor, digitizing the image, and passing the image to computer memory. An adaptive segmentation module was used to calculate the appropriate segmentation level for each image. The segmentation level could be calculated from a region, or window, of the image or from the entire image. Gray–level histograms were developed either from the prior image (entire image–based segmentation level) or from the selected region (window–based segmentation level). Histogram–based segmentation gave some measure of adaptivity with respect to the ambient illumination. The histogram represented the actual pixel level intensity found in the image. An external specification file provided the desired cumulative percentage goal for segmentation. The cumulative percentage goals were ambient light level dependent and were adjusted by the operator prior to starting. The segmentation levels were based on the actual pixel value rather than the percentage; the histogram was used to map the desired cumulative percentage to a pixel value.

After determining the appropriate segmentation levels for the image, processing shifted from whole–image to line–by–line processing. Each line in the image was segmented using the segmentation levels determined in the adaptive segmentation module. After segmentation, a 7 × 7 low–pass filter was applied to the image, and a blob analysis procedure was performed.

The segmentation module utilized the levels calculated by the adaptive segmentation module. The segmentation module operated on the active processing region (i.e., window or entire image) defined by the adaptive segmentation module. With a monochrome image, it was relatively simple: if the pixel value was above the adaptive gray level, then the pixel was classified as part of the guidance class:

$$\left.\begin{aligned} p_C(i,j)=1 \\ p_C(i,j)=0 \end{aligned}\right\} \quad \begin{aligned} &\text{if } p(i,j) > p_{gsl} \\ &\text{if } p(i,j) < p_{gsl} \end{aligned} \qquad (1)$$

After segmenting the image, a low–pass filter was used to remove noise. The blob analysis procedure was not particularly noise sensitive. However, each new blob encountered was assigned a block of memory for processing; with noisy images, memory limitations became a restriction.

Blob analysis treats connected pixels of the same image classification as a single object. In the scene, the inter–row space represented a single, connected object oriented along the axis of motion of the combine. Blob analysis was used to detect the largest connected region in the image and to calculate the appropriate characteristic values for the object. A run length encoding (RLE) procedure was used to reduce the individual pixels from a series of location and intensity values to a segment with a known start location and length. Run length encoding inherently evaluates the connectivity along the axis of the encoding. Each encoded segment was checked against the segments from the previous lines of the image for overlap. If the current segment overlapped a segment from the previous image line, then the current segment was considered to be part of the same blob. If the segment did not overlap a previous segment, then the segment was assigned a new blob identification number. Each active blob was checked to see if it overlapped another blob; overlapping blobs were reassigned the same identification number. Initially, the algorithm only considered directly contiguous segments to be part of the same blob. The inter–row space had a decidedly longitudinal (along the axis of travel) trend; occasionally, leaves connected the crop rows together and disrupted the inter–row space. The blob analysis module was modified to allow a user–adjustable dilation factor, which considered blobs within the dilation factor to be part of the same blob. The dilation factor could be set independently in the vertical and horizontal directions. Typically, the dilation factor was 5 to 8 times larger in the vertical direction than in the horizontal direction.

The blob analysis procedure evaluates features in the image as objects rather than independent pixels or lines in the image. In several other machine vision guidance algorithms, each line was evaluated independently. There was no relationship between the current line and the previous line, and feature extraction did not require processing every line in the image. With the most successful algorithm developed, connected series of pixels represent the same object or feature. The inter–row space has a decidedly longitudinal or image vertical trend to it; skipping lines or portions of the image would reduce the pixel connectivity. Experience with the system showed that the rows immediately adjacent to the center row were more visible at the bottom of the image than the top; early termination would increase the likelihood of selecting the wrong row. The dilation factor connected nearby objects that represented the same features, enhancing

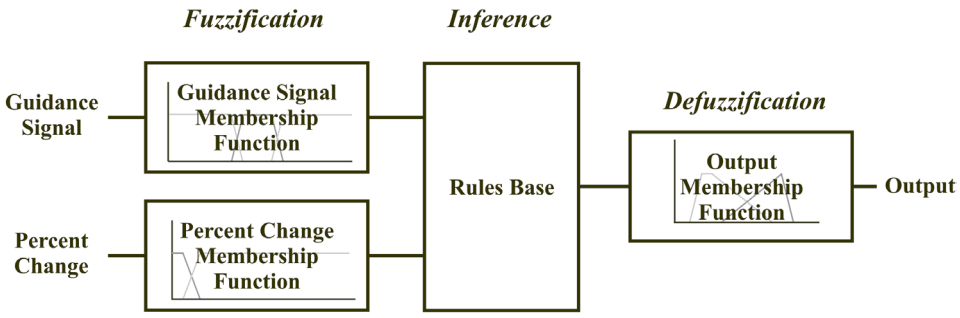

Figure 4. Schematic of the fuzzy quality evaluation module.

detection of the correct row. The dilation factor ranged from 0 to 2 horizontally to 5 to 10 vertically.

To preserve feature connectivity, the entire image was processed. The size of the processed region influenced the algorithm processing rate. With the blob analysis procedure, the connectivity of the RLE segments determined which segments were classified as part of the same object. The crop rows have a decidedly longitudinal trend, which caused the inter–row space to have a trend along the axis of motion (along the vertical axis of the image). Early termination would minimize the vertical trend and increase the chance of detecting the wrong row. Increasing the size of the processed region affects speed in two ways: (a) each additional line in the image had to be segmented, filtered and processed, and (b) the connectivity of the active blobs had to be evaluated on a line–by–line basis. Due to the dilation factor, each vertical line processed required scanning an additional 5 to 10 image lines. Processing the entire image was much slower than processing only the reduced region of interest.

The blob statistics were calculated after processing the entire image. The area, centroid, form factor, perimeter, and composite index were calculated for each blob. A linear regression was performed on the blob with the largest composite index. The developer could select whether to use the centroid or regression results for guidance. Typically, better results were obtained with the centroid than with the raw regression results.

The algorithm tracked the center inter–row space. During testing, especially in weaker stands of corn or dense leaf canopies, the system occasionally selected a false inter–row space. Improper row selection caused the guidance system to veer suddenly and attempt to center the combine on an incorrect row. A fuzzy logic module was inserted between the blob calculations and the vehicle controller to determine if the algorithm output was appropriate for the center row (fig. 4). The two inputs for the fuzzy evaluation module were the guidance signal and the absolute value of the percent change in the guidance signal. The guidance signal was used to ensure that the value was within a reasonable range. From experience, the output did not vary significantly from image to image. The input and output membership functions are shown in figure 5. The membership functions classify the input and output, while the rules base determines which rules apply. The output from the module was a binary acceptance rating. If the output was acceptable, the results were used for guidance. If the results were not acceptable, then guidance was based on the results from the most recent acceptable image.

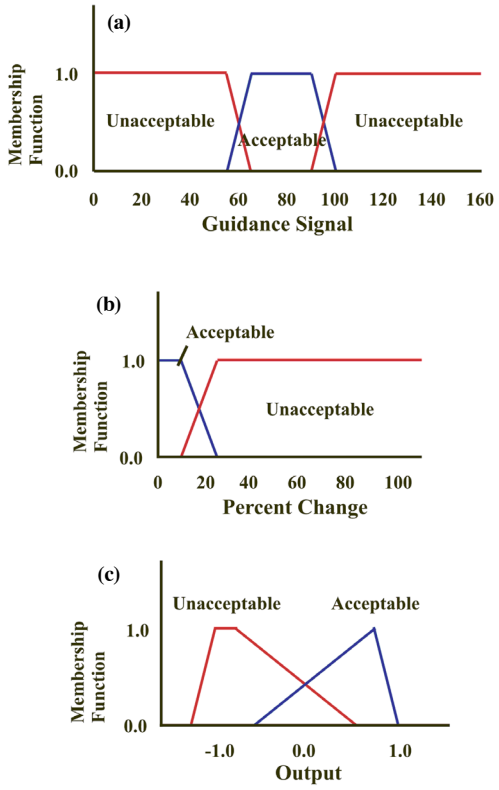

Figure 5. Fuzzy quality evaluation membership functions: (a) guidance signal, (b) percent change in guidance signal, and (c) output.

The guidance signal from the fuzzy quality evaluation module was converted to a desired wheel angle by a PID controller:

$$e_i = (GS_{goal} - GS_{act}) \tag{2}$$

$$\delta_d = K_p e + K_i \int e dt + K_d \frac{de}{dt} \tag{3}$$

The PID gains were tuned to reduce overshoot and maximize tracking accuracy. Best performance was obtained with gains of K_p = 1.35, K_i = 0.075, and K_d = 0.15. The calculated guidance signal was sent to the separate steering controller via an RS–232 serial link. The steering controller and the guidance algorithm were asynchronous; the separate controller ran at a higher update rate than the main guidance system.

EXPERIMENTAL RESULTS

The algorithm was evaluated both in the laboratory and in the field. Sample images were collected and characterized during harvest to evaluate the relative contrast in the image. The combine was tested in the field in an observer mode, with the processing system active, but the vehicle under manual control. In addition, the system was used to guide the combine under typical field conditions.

EXPERIMENTAL SYSTEM

A Case 2188 combine harvester was used as the guidance research platform. During data collection, the axial–flow combine was equipped with an 8–row corn head. The steering system of the combine was modified to include an electrohydraulic valve, an additional steering cylinder, and a dedicated steering controller. A master kill switch for the electrohydraulic valve was provided for the operator, allowing the operator to interrupt steering control for safety reasons. A supplemental electrical system was added to handle the additional guidance electronics. A 450 MHz Pentium–based computer was installed in the cab of the combine for image processing and guidance. A Trimble 4400 RTK GPS receiver was used to record the position of the vehicle during guidance.

A single camera was installed on the centerline of the combine cab. The camera height and orientation were adjustable; however, the camera was normally oriented to view directly ahead of the combine at a slight downward angle for the duration of the tests. The camera was located 3.2 m above ground (126 in), 1.5 m (60 in) ahead of the front axle, and with a camera down angle of 15°.

The primary image sensor for this project was a Cohu 2100 monochrome camera. The camera has a maximum resolution of 752 × 582 pixels (horizontal × vertical) and automatic gain control (AGC). The AGC reduced the effect of moderate changes in illumination but could not compensate for drastic changes. Images were recorded using both analog videocassette recorders and an ImageNation PXC–200 color frame grabber.

The image collection system was used to collect video over a selection of typical central Illinois cornfields. Fields 1, 2, and 3 were University of Illinois research plots; field 4 was owned and managed by a research cooperator. The algorithm was tested and developed on four fields totaling 24.0 ha (58.9 acres) (table 1). Images were recorded simultaneously with the steering and position data.

CONTRAST STUDY

Two representative sequences were analyzed from video collected during the harvest season. The images were captured at 8–bit resolution, and the average intensity levels within the image were analyzed. The gray–level statistics for the crop and non–crop regions in each image are presented in table 2.

Table 1. Field summary, harvest dates, and yield for data collection and evaluation.

Field	Location	Harvest Date (year 2000)	Area, ha (acres)	Yield, t/ha (bu/A)
1	Urbana, Ill.	19 to 28 Sept.	4.6 (11.2)	8.29 (119.9)
2	Urbana, Ill.	2 Oct.	6.8 (16.6)	8.30 (120.0)
3	Urbana, Ill.	10 Oct.	3.3 (8.2)	8.65 (125.1)
4	Fairmont, Ill.	25 to 31 Oct.	13.9 (34.1)	8.88 (128.3)

Table 2. Gray–level characterization of the crop and inter–row space in sample harvest images.

	Inter–Row Space		Crop	
Sequence	Mean	Deviation	Mean	Deviation
A	57.14	18.58	203.13	55.80
B	65.23	23.61	121.09	29.55

There was a clear separation between the two classes. A paired t–test for samples with unknown and equal variances was used to evaluate class separation. The differences between the crop and inter–row regions were statistically significant ($\alpha = 0.05$). The average crop gray level was significantly higher than the average gray level in the inter–row space. The inter–row space appeared as a dark component in the image and had a lower average gray level. Portions of the crop canopy obscured or partially obscured the inter–row space of some images. Intermingling of the canopy and row space in the images tended to increase the average and standard deviation of the inter–row gray level.

The mean values for both classes were widely spaced, which facilitated reliable segmentation. The class gray levels were not consistent sequence to sequence, which implied that an adaptive segmentation routine was required. The contrast evaluation results indicated that accurate segmentation and classification were possible.

STEERING EVALUATION

The number and magnitude of changes required by the controller is an indication of how much "effort" the controller is exerting to follow a desired pathway. The combine was first operated in observer mode, with the guidance system active but with a human operator controlling the steering. The system was then operated with the guidance system active and controlling the steering of the combine. The steering performance of the system is shown in table 3 and figure 6. The results shown are represent the various situations encountered at the test sites.

The average and standard deviation values indicate how much difference there was between the manual steering angle and the controller–indicated predicted steering angle. These values were most relevant for the observer mode trials, in which the human operator provided a baseline measurement (actual angle) for comparison. In the guidance system trials, the actual measurement reflects the current steering angle when a new steering command was provided. As shown in table 3, the observer mode trials indicate that the actual angle

Table 3. Steering results from sample observer mode and automatically controlled guidance passes.

	Actual Angle (deg.)		Predicted Angle (deg.)		Steering Angle Change, RMS (deg.)	
	Avg.	SD	Avg.	SD	Actual	Desired
Observer mode	2.60	5.05	4.13	5.05	5.27	5.53
Guidance trial A	1.61	3.21	5.10	3.28	2.89	2.88
Guidance trial B	1.86	2.52	5.88	2.57	4.68	4.47

Figure 6. Observer mode steering performance versus distance: (a) observer mode with a human operator, and (b) guidance system active.

(2.60˚) and desired angles (4.13˚) were similar, and the error was relatively low (–1.53˚). The operator manually corrected the position of the combine to achieve maximum harvesting efficiency. With the guidance system trials, there was a larger difference between the actual (steering controller) and desired (guidance system) angles. The difference stems partially from the design of the system, in which the asynchronous steering controller continually adjusts the steering angle to match the most recent signal from the guidance system. The steering angle returned to the system is the current steering angle, although the controller may not have reached the desired steady–state value by the time the steering angle was recorded.

The change in angle RMS value provides a better indication of how much "effort" was required to control the pathway of the vehicle. The change in angle is the change in angle from one cycle of the guidance system to the next. In the observer mode trial, the actual (operator) effort and controller effort were very similar. This implies that the controller was no less efficient than a typical human operator. The two guidance trials were from a different field and cannot be directly compared to the observer mode; however, in both cases, the average accumulated error was less than in the observer mode trial. The difference between the observer and guidance trials cannot be separated from the differences due to the crop and field arrangement.

Two sample plots of steering angle versus distance are shown in figure 6. In both of the trials shown, the predicted and actual steering angles appear to be highly correlated. The predicted steering angle tended to lag the operator's actual angle. The actual angle driven by the operator influenced the image scene, which partially explains the lagging effect. The system was responding to changes in the image.

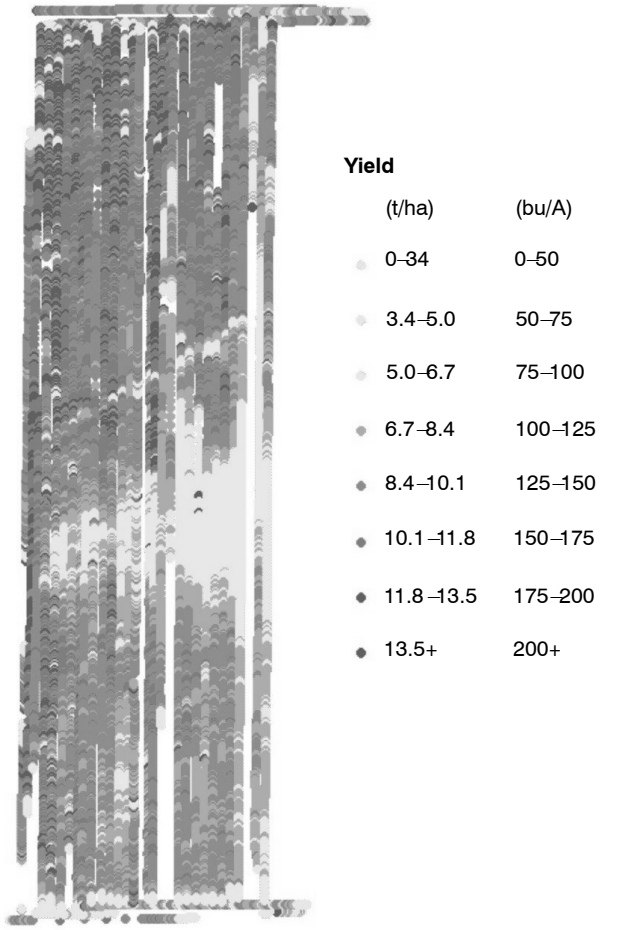

Figure 7. Yield map from the field used for experimental guidance.

Experimental Guidance

The guidance system was used to automatically steer the combine while actively harvesting a typical Illinois field. The operator remained with the vehicle both for safety reasons and to manually adjust the combine settings (header, threshing, etc.). The combine was manually operated in the head rows and approximately aligned with the rows before activating the guidance system. The combine was able to successfully harvest the field during both day and night. The standard combine lights provided the illumination for automatic guidance at night.

Experimental guidance work was carried out on field 4 from 25 to 31 October 2000. The field was roughly rectangular with the rows aligned north to south and with a waterway serving as the eastern border. The average yield for the field was 8.61 t/ha (128.0 bu/A), with a typical range of 4.84 to 13.19 t/ha (72 to 196 bu/A), as shown in figure 7. A small drainage ditch split the field into a northern third and a southern two–thirds, with yields generally lower in the southern portion. In a few areas, the yield dropped into the 1.35 to 2.02 t/ha (20 to 30 bu/A) range. The crop had little lodging and was largely undamaged.

The maximum operating velocity of the combine was limited by the speed of the image processing system. The maximum velocity was 1.3 m/s (3.0 mph). Even after

reducing the size of the processing window, the algorithm was still relatively slow (approximately 2.0 Hz).

The test site was outside the range of the radio link from the RTK GPS base station to the combine GPS receiver. Since there were no known benchmarks at the test site, the absolute accuracy of the system could not be assessed. For this application, however, the relative repeatability of the measurements was more important. GPS output was recorded for approximately 2 min with the system stationary. The GPS data were converted from latitude and longitude to Universal Transverse Mercator (UTM) projection to simplify measurements. At the Fairmont site, the 1–σ dispersion for the GPS system was 11.0 cm (4.33 in.) (northing) and 1.38 cm (0.54 in.) (easting).

The relative accuracy of the system was 0.6 cm (0.24 in.) with a 13.3 cm (5.23 in.) standard deviation (table 4). The average daytime accuracy of the system was 0.3 cm (0.12 in.) with a 13.3 cm (5.23 in.) standard deviation. The average nighttime accuracy of the system was –2.4 cm (0.94 in.) with a 12.9 cm (5.07 in.) standard deviation. The actual row positions were not known. A second–order spline fit was used to parameterize the rows from the position data, with R^2 greater than 0.975 for each of the runs. The indicated average accuracy is a measure of how well the model represented the data; the deviation measurements provide a good indication of how well the system could track a given path.

The dispersion of the GPS and the indicated accuracy of the system were similar orders of magnitude. A standard pooled t–test was performed to test the hypothesis that the indicated accuracy of the system was statistically different from the GPS dispersion. The results, as shown in table 5, indicate that system accuracy and GPS accuracy were not statistically different at the 5% level (t = 2.77). The guidance system was as accurate as the recording information available.

In the field, system performance and crop condition appeared to be related. In moderate– to high–yielding areas, the system rarely encountered problems. In low–yielding areas, the algorithm could not reliably locate the crop rows. The algorithm utilizes the rows in view to determine the appropriate steering command for the vehicle; missing or damaged plants make it difficult to detect the row structure.

In the field, the performance of the guidance system was affected by crop condition; in areas of low or sparse crop, the system did not perform well. To test the hypothesis that crop condition and performance were related, the output from the fuzzy quality evaluation module was compared with yield. The output from the fuzzy evaluation module was a value of acceptable or unacceptable depending on the guidance signal value and change in guidance signal. If the yield and guidance system performance were related, then the yield associated with regions of acceptable performance would be higher than the yield associated with regions where the performance was unacceptable.

Table 4. Accuracy of the system as compared to a second–order spline fit of the data.

Sequence	Average (cm)	SD (cm)	RMS (cm)
Day	0.3	13.3	13.3
Night	2.4	12.9	13.1
Overall	0.5	13.3	13.3

Table 5. Statistical significance of the indicated accuracy versus the deviation of the GPS position recording equipment.

Comparison	t
Daylight operation versus GPS	–1.53
Night operation versus GPS	1.41
Daylight versus night operation	–2.24

The average yield for the acceptable and unacceptable regions was calculated for the test runs, and summaries are provided in table 6. There was a statistically significant yield difference between the acceptable and unacceptable regions. The results presented in table 6 indicate that yield and acceptability are related. In general, yield in the acceptable region was higher than yield in the unacceptable region. The yield in the unacceptable region was higher in three test runs, which suggests that crop condition (as represented by yield) is not the only factor that governs the performance of the algorithm.

DISCUSSION

The algorithm developed was successfully used to control the steering of the combine in the field. The system guided the combine through a typical field at a level of accuracy comparable with manual steering.

The high–mounted camera location enhanced contrast in the image. Previous experience with a low head–mounted camera (Benson, et al., 2000a, 2000b) showed that segmentation was possible only when the crop shadow created an artificially high contrast region in the image. The high–mounted camera images contained sufficient contrast to allow successful segmentation of the image under most conditions. Although the images contained sufficient contrast to allow segmentation during both day and night operation, lighting and shadows remain an issue.

While the algorithm was capable of moderate performance, processing speed was a significant limitation. With reduced–size images and limited data recording, the system ran at 2.0 Hz. The vehicle continued to move during the time between vehicle controller updates. The slower the vehicle controller, the further the vehicle moved before the next control signal was calculated. The slower the controller, the more processing errors (i.e., incorrect row selection or segmentation errors) and image errors (missing plants or row) affected the system.

The fuzzy evaluation system and the relatively slow processing speed magnified the effect of image processing errors. In the event of an image processing error, the output was disregarded and the output from the previous iteration was used. In the field, gaps typically occured in several sequential images. The net effect was that the same controller output was held for several iterations, which typically translated to one second or more. When a proper image was received, a relatively large steering correction was then required to bring the vehicle back on course. With a faster processing system, new guidance signals could be calculated more rapidly, and the overshoot would be minimized.

The limited processing speed forced the operator to reduce the speed of the combine. Typical manual operating speeds ranged from 1.8 m/s (4.0 mph) to 2.7 m/s (6.0 mph), depending on field conditions. With the guidance system

Table 6. Statistical significance of the acceptability as compared to crop yield.

Run ID	Yield (bu/A) Accepted[a]	Not Accepted[b]	Z
Day	128.31	119.63	8.02
Night	111.89	106.13	3.62
Total	126.9	118.3	7.12

[a] Yield when fuzzy quality module indicated image processing output was acceptable.

[b] Yield when fuzzy quality module indicated image process output was not acceptable.

active, the maximum speed of the combine was limited to 1.3 m/s (3.0 mph).

An improvement in processing speed would improve the field performance of the system. The algorithm used a blob analysis procedure that required evaluating the pixel connectivity. For every line in the image, the connectivity of each blob had to be determined. Evaluating the connectivity increased the processing time. Improvements in coding efficiency, dedicated image processing hardware, or a simpler processing method could speed processing. The current speed limitation is a short–term restriction, not a long–term barrier to future implementation.

In the field, the crop condition clearly affected the performance of the system. Simply stated, if there is no crop, then a machine vision system cannot provide a guidance signal. Every time a low spot or weak crop stand was encountered, the performance of the system began to deteriorate.

Conclusion

A machine vision–based guidance system was developed and evaluated under both laboratory and field conditions. The guidance system utilized a single monochrome camera located above the cab of the combine and mimicked the steering method used by the operator. The system was able to harvest 4.7 ha (11.6 acres) of corn both during the day and at night, successfully steering the combine without intervention by the operator. The indicated accuracy of the guidance system was the same as the accuracy of the GPS system used to record the position of the combine. Crop condition and yield affected the performance of the algorithm. Field trials demonstrated that a machine vision–based guidance system can assist the operator.

Acknowledgements

The research was supported by CNH Global NV. Funding for Eric Benson was provided by a fellowship from the University of Illinois College of Agricultural, Consumer, and Environmental Sciences. The authors would also like to thank Francisco Rovira Mas, Dr. Jeffery Will, Larry Meyer, Marcia Mohr, and Mark Mohr for their contributions to the project.

References

Bell, T. 2000. Automatic tractor guidance using carrier–phase differential GPS. *Comput. Elect. Agric*. 25(1/2): 53–66.

Benson, E. R., J. F. Reid, Q. Zhang, and F. A. C. Pinto. 2000a. An adaptive fuzzy crop edge detection method for machine vision. ASAE Paper No. 001019. St. Joseph, Mich.: ASAE.

Benson, E. R., J. F. Reid, and Q. Zhang. 2000b. Development of an automated combine guidance system. ASAE Paper No. 003137. St. Joseph, Mich.: ASAE.

Callaghan, V., P. Chernett, M. Colley, T. Lawson, J. Standeven, M. Carr–West, and M. Ragget. 1997. Automating agricultural vehicles. *Industrial Robot* 24(5): 364–369.

Fitzpatrick, K., D. Pahnos, and W. V. Pype. 1997. Robot windrower is first unmanned harvester. *Industrial Robot* 24(5): 342–348.

Gan–Mor, S., and R. L. Clark. 2001. DGPS–based automatic guidance – Implementation and economical analysis. ASAE Paper No. 011192. St. Joseph, Mich.: ASAE.

Gerrish, J. B., B. W. Fehr, G. R. Van Ee, and D. P. Welch. 1997. Self–steering tractor guided by computer vision. *Applied Eng. in Agric*. 13(5): 559–563.

Hague, T., and N. D. Tillett. 1995. Navigation and control of an autonomous horticulture robot. *Mechatronics* 6(2): 165–180.

Keicher, R., and H. Seufert. 2000. Automatic guidance for agricultural vehicles in Europe. *Comput. Elect. Agric*. 25(1/2): 169–194.

Jahns, G. 1997. Automatic guidance of agricultural field machinery. In *Proc. Joint International Conference on Agricultural Engineering and Technology Exhibition*, 70–79. Dhaka, Bangladesh. 15–17 December. St. Joseph, Mich.: ASAE.

Nieminen, T. J., and M. Sampo. 1993. Unmanned vehicles for agricultural and off–highway applications. SAE Paper No. 932475. Warrendale, Pa.: SAE.

Ollis, M. 1997. Perception algorithms for a harvesting robot. PhD diss. Pittsburgh, Pa.: Carnegie–Mellon University, The Robotics Institute.

Ollis, M., and A. Stentz. 1996. First results in vision–based crop line tracking. In *Proc. IEEE International Conference on Robotics and Automation*, 951–956. Piscataway, N.J.: IEEE.

Palmer, R. J., and S. K. Matheson. 1988. Impact of navigation on farming. ASAE Paper No. 881602. St. Joseph, Mich.: ASAE.

Reid, J. F., Q. Zhang, N. Noguchi, and M. Dickson. 2000. Agricultural automatic guidance in North America. *Comput. Elect. Agric*. 25(1/2): 154–168.

Tillett, N. D., T. Hague, and J. A. Marchant. 1998. A robotic system for plant–scale husbandry. *J. Agric. Eng. Research* 69(2): 169–178.

Van Zuydam, R. P. 1999. A driver's steering aid for an agricultural implement based on an electronic map and real–time kinematic DGPS. *Comput. Elect. Agric*. 24(3): 153–156.

Wilson, J. N. 2000. Guidance of agricultural vehicles – A historical perspective. *Comput. Elect. Agric*. 25(1/2): 3–9.

Nomenclature

$A(k)$ = area of blob k
e_i = error, or difference between the ideal guidance signal and the actual guidance signal, at iteration i
$CI(k)$ = composite index of blob k
$FF(k)$ = form factor of blob k
$GS(i)$ = guidance signal calculated from the image at iteration i
GS_{goal} = guidance signal goal, dictated by the camera location
i = row index
j = column index
k = blob index
K_d = derivative vehicle controller gain
K_i = integer vehicle controller gain

K_p = proportional vehicle controller gain
m_{edge} = parameterized regression slope of the crop edge
N_{scan} = number of scan lines used to develop the line profile
N_{int} = interval between scan lines
$P(k)$ = perimeter of blob k
$p(i,j)$ = pixel monochrome level at a given row and column
$p_c(i,j)$ = pixel segmentation class
P_{gsl} = pixel monochrome segmentation level
X_c = centroid of blob k
δ_d = desired wheel angle (°)